



Revista Portuguesa de Cardiologia

Portuguese Journal of **Cardiology**

www.revportcardiol.org



ORIGINAL ARTICLE

Noninvasive anatomical and functional assessment of coronary artery disease



Vítor Ramos^{a,*}, Nuno Bettencourt^b, Jennifer Silva^b, Nuno Ferreira^b,
Amedeo Chiribiri^c, Andreas Schuster^d, Adelino Leite-Moreira^{e,f},
José Silva-Cardoso^{e,f}, Eike Nagel^c, Vasco Gama^b

^a Cardiology Department, Hospital de Braga, Portugal

^b Cardiology Department, Centro Hospitalar de Vila Nova de Gaia/Espinho, Portugal

^c Division of Imaging Sciences and Biomedical Engineering, King's College London, London, United Kingdom

^d Department of Cardiology and Pneumology and Heart Research Centre, Georg-August-University, Göttingen, Germany

^e Cardiology Department, Centro Hospitalar de S. João, Portugal

^f Faculty of Medicine, Porto University, Portugal

Received 23 July 2014; accepted 10 October 2014

Available online 1 April 2015

KEYWORDS

Coronary artery disease;
Fractional flow reserve;
Computed tomography angiography;
Cardiac magnetic resonance myocardial perfusion imaging;
Integrated assessment

Abstract

Introduction and Objective: In suspected coronary artery disease (CAD), invasive coronary angiography (ICA) is traditionally the diagnostic tool of choice. However, patients often have no significant disease. Moreover, assessment of fractional flow reserve (FFR) has been shown to have prognostic implications. Recently, coronary computed tomography angiography (CTA) and cardiac magnetic resonance (CMR) myocardial perfusion imaging (CMR-Perf) have gained increasing attention through their accurate anatomical and functional assessment, respectively. We studied the added value of integrating these tests (CT+CMRint) in the diagnosis of CAD, with FFR as the reference standard.

Methods: We included 101 patients consecutively referred for outpatient assessment of CAD who underwent CTA and CMR-Perf prior to ICA with FFR assessment. Lesions were considered positive by CT+CMRint only if positive in the two tests alone. The mean follow-up was 2.9±0.6 years.

Results: All patients completed the study protocol without adverse effects. Forty-four patients had CAD by FFR. CTA had excellent sensitivity and negative predictive value (100%) but, as expected, its specificity and positive predictive value were lower (61% and 67%, respectively). Diagnostic accuracy by FFR was 78% for CTA, 88% for CMR-Perf and 92% for CT+CMRint. Regarding diagnostic accuracy, CT+CMRint showed statistically significant superiority (AUC=0.917, 95% CI 0.845–0.963) compared with CTA (AUC=0.807, 95% CI 0.716–0.879, p=0.0057) or CMR-Perf (AUC=0.882, 95% CI 0.802–0.938, p=0.0398) alone. Regarding prediction of revascularization, the integrated protocol maintained its superior performance.

* Corresponding author.

E-mail address: vglramos@gmail.com (V. Ramos).

PALAVRAS-CHAVE

Doença coronária;
Reserva fracional funcional;
Angio TC cardíaco;
Estudo de perfusão por ressonância magnética cardiovascular;
Avaliação integrada

Conclusions: CT+CMRint showed superior diagnostic accuracy and could thus lead to a considerable reduction in invasive procedures for CAD diagnosis, with less risk and greater patient comfort.

© 2014 Sociedade Portuguesa de Cardiologia. Published by Elsevier España, S.L.U. All rights reserved.

Avaliação não-invasiva, anatômica e funcional, da doença coronária**Resumo**

Introdução e Objetivo: Na suspeita de doença coronária, o cateterismo cardíaco (CC) é tradicionalmente o exame escolhido mas, frequentemente não surge doença significativa. Também, a avaliação da reserva fracional funcional (RFF) tem implicações prognósticas. Recentemente, tanto o angioTAC (CTC) como a ressonância magnética cardiovasculares (RMC) assumiram o seu lugar pela excelente acuidade, respetivamente, na avaliação anatômica e funcional de doença coronária. Foi nosso objetivo investigar o valor adicional da sua integração, tendo a RFF como referência.

Métodos: 101 pacientes consecutivamente referenciados do ambulatório por suspeita de doença coronária foram submetidos a CTC e a RMC previamente ao CC. A avaliação integrada (CTC+RMCint) foi considerada positiva se anormalidades presentes simultaneamente nos dois testes. O período médio de *follow-up* foi de $2,9 \pm 0,6$ anos.

Resultados: Todos os pacientes completaram o protocolo sem adversidades. Doença coronária por RFF ocorreu em 44 pacientes. A CTC demonstrou uma excelente especificidade e VPN (100%) mas, como esperado, baixa especificidade e VPP (61 e 67%). A acuidade diagnóstica foi de 78% para a CTC, 88% para a RMC e 92% para a CT+CMRint. O protocolo integrado demonstrou superioridade estatisticamente significativa para prever doença coronária definida por RFF (AUC=0,917, IC 95% 0,845-0,963) quando comparado com a CTC (AUC=0,807, IC 95% 0,716-0,879, $p=0,0057$) e RMC (AUC=0,882, IC 95% 0,802-0,938, $p=0,0398$) isoladamente. Tal manteve-se quando considerada a revascularização no *follow-up*.

Conclusão: A CTC+RMCint demonstrou acuidade diagnóstica superior o que poderá levar à diminuição da realização de CC diagnósticos, com menor risco e maior conforto para o paciente.

© 2014 Sociedade Portuguesa de Cardiologia. Publicado por Elsevier España, S.L.U. Todos os direitos reservados.

Introduction

In suspected coronary artery disease (CAD), invasive coronary angiography (ICA) is traditionally the diagnostic tool of choice. However, patients undergoing this exam often have normal coronary arteries or no significant disease, but the risks and costs associated with this invasive approach are significant.¹ The rapid evolution of computed tomography (CT) after the introduction of multidetector scanners has allowed noninvasive assessment of coronary anatomy. CT angiography (CTA) has expanded in clinical practice and, as expected from an anatomical study, it is associated with high sensitivity and negative predictive value (NPV).²⁻⁴ Nevertheless, its ability to discriminate the degree of stenosis is limited, mainly due to artefacts resulting from calcified and complex lesions and also due to inherent cardiac motion.^{5,6} Thus, CTA is currently mainly reserved for patients with a low likelihood of CAD.²⁻⁴

The main limitation of anatomical assessment is that correlation with functionally relevant disease is not straightforward.^{7,8} The length, number and tortuosity of lesions, as well as collateral flow, influence the

hemodynamic significance of coronary lesions.⁹ Fractional flow reserve (FFR) distal to the lesion on ICA has prognostic implications and influences the decision to revascularize.^{10,11} Myocardial perfusion studies enable functional assessment, and cardiac magnetic resonance (CMR) perfusion imaging has also been adopted in clinical practice, with high diagnostic accuracy.¹²⁻¹⁵ Another advantage of CMR perfusion imaging is its versatility and ability to provide alternative diagnoses.¹⁶

The prospect of incorporating anatomical and functional evaluation in a noninvasive approach is attractive, but it has yet to find a place in clinical practice. The added value of coronary MR angiography over CMR perfusion imaging is doubtful, mainly due to limitations arising from spatial resolution, scan duration and artefacts.^{17,18} Hybrid imaging techniques such as positron emission tomography (PET) and CTA, or CTA combined with single photon emission computed tomography (SPECT) myocardial perfusion scintigraphy, have shown interesting results, though limited by the small number of studies and lack of access in clinical practice.^{19,20} Several groups, including a recent multicenter study, have consistently shown the added value of

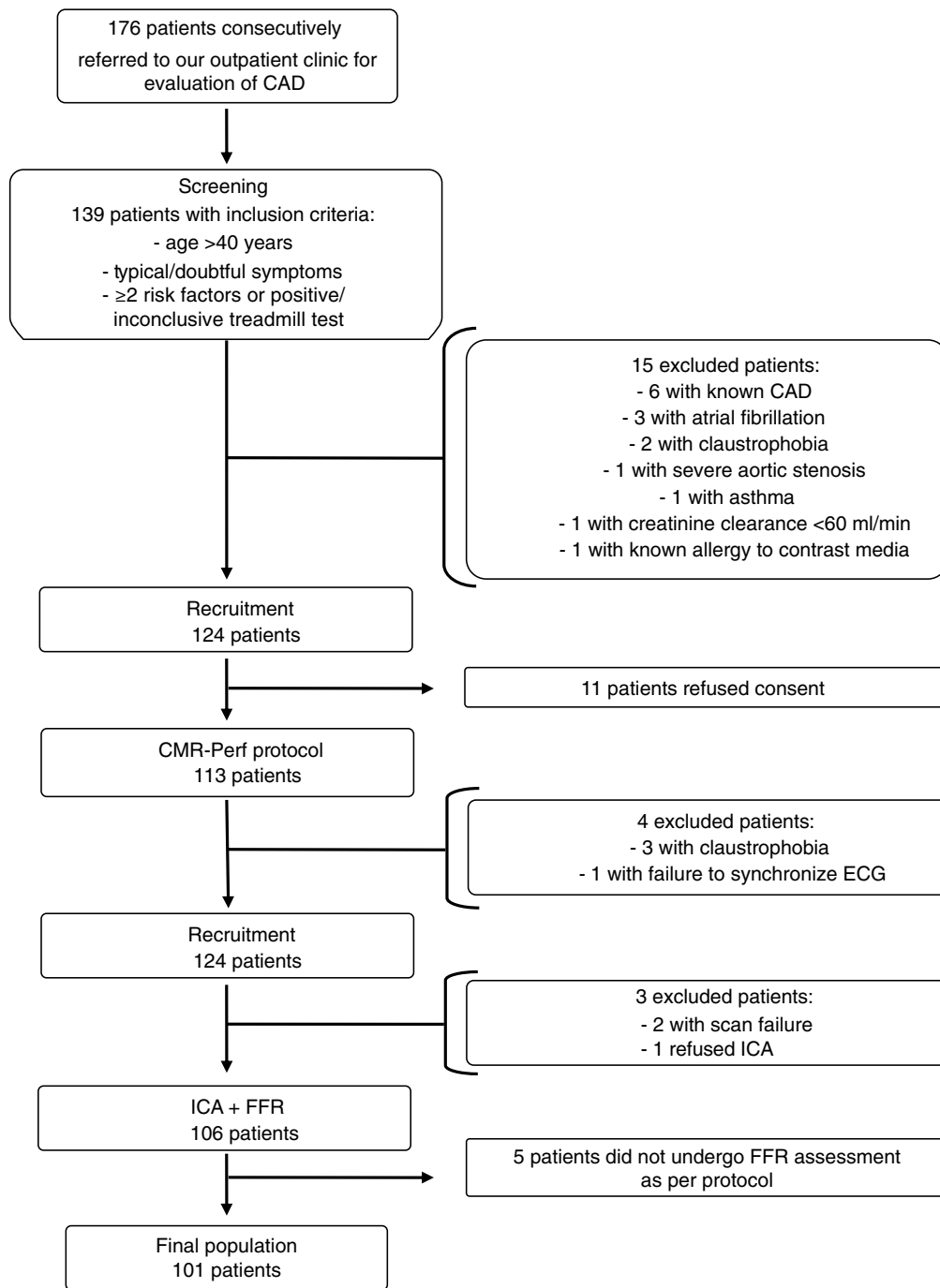


Figure 1 Study flow-chart and reasons for exclusions. CAD: coronary artery disease; CMR-Perf: cardiac magnetic resonance perfusion imaging; FFR: fractional flow reserve; ICA: invasive coronary angiography.

integrating data from CT perfusion (CTP) imaging with CTA, mainly because of higher specificity and positive predictive value (PPV).²¹⁻²³ CTP studies follow the general principles of CMR perfusion imaging, although they are at an early stage of development and only provide moderate diagnostic value.²⁴

Our aim was to study the added value of integrating the two current reference techniques for noninvasive anatomical and functional assessment of CAD, CTA and CMR perfusion imaging, respectively. A population with suspected CAD who would normally be referred for ICA was studied, but with

additional assessment by FFR, according to the current indications.²⁵

Methods

Population and study design

The study population included 176 patients consecutively referred to our outpatient cardiology clinic for assessment of CAD between January 2010 and November 2011. Inclusion

criteria were age >40 years, symptoms compatible with CAD and ≥ 2 cardiovascular risk factors or positive or inconclusive treadmill test. Exclusion criteria were clinical instability, known CAD, significant valvular heart disease, atrial fibrillation, pregnancy, creatinine clearance <60 ml/min and standard contraindications for CMR, adenosine and contrast media. Figure 1 summarizes the study design and exclusion criteria.

The final population consisted of 101 individuals with an intermediate to high pretest probability (Table 1). The local research ethics committee approved the study protocol and written informed consent was obtained from all patients.

CTA and CMR perfusion imaging studies were performed in the week previous to ICA. Patients were instructed to refrain from smoking, consuming coffee or tea, or taking theophyllines, beta-blockers, calcium antagonists or nitrates in the previous 24 hours. Readers were blinded to the clinical information and other test results. The decision for coronary revascularization was the responsibility of the patients' attending clinicians, who were not bound by standard FFR criteria.

Computed tomography angiography protocol

The CTA protocol used a 64-slice SOMATOM Sensation 64 scanner (Siemens Medical Solutions, Forchheim, Germany) as part of a previously described comprehensive stress-rest protocol²² optimized to study stress CTP.

The study began with a prospective ECG-gated acquisition without contrast (120 kV, 190 mAs) for coronary calcium scoring, which was used to guide subsequent acquisitions. Infusion of adenosine at 140 $\mu\text{g}/\text{kg}/\text{min}$ was then initiated. After at least 3 min, the first pass of iodinated contrast (Ultravist, iopromide 370 mg/ml, Bayer Healthcare, Leverkusen, Germany) injected at 4.5 ml/s, was registered by retrospective acquisition with tube current modulation (maximum power 60–65% of the R-R interval) and bolus-tracking (150 HU threshold, delay 4 s.) The collimation achieved was 64 mm \times 0.6 mm. The full tube current was adjusted to body mass index (600 mAs for 20–30 kg/m², 800 for >30 kg/m² and 400 for <20 kg/m²).

Immediately after this acquisition, adenosine infusion was suspended. If heart rate exceeded 65 bpm (44 patients), intravenous boluses of fractionated metoprolol (5–20 mg) were administered for a target rate of ≤ 60 bpm. Five minutes before CTA all patients were given 0.05 mg of sublingual nitroglycerin. Ten minutes after the stress acquisition, a new prospective ECG-gated acquisition was performed (65% of the R-R interval, 100 kV, 110 mAs). The timing and amount of contrast used were similar to the stress acquisition.

Computed tomography analysis

Although the study was optimized for CTP, as this was a concomitant target of our research center, only coronary angiography data were analyzed for the purposes of this study.²² Acquisitions both under stress and at rest were reconstructed using a soft kernel (Siemens B25f) with 0.6 mm slice thickness. The compiled data were blinded and sent to a postprocessing station (Aquarius, TeraRecon Inc., CA, USA) for interpretation by two cardiologists experienced

Table 1 Clinical characteristics of the study population (n=101).

| <i>Baseline characteristics</i> | |
|--|-----------------------------|
| Male | 68 (67%) |
| Age, years (min-max) | 62 \pm 8.0 (41–79) |
| Body mass index, kg/m ² | 28.0 \pm 4.45 (19.9–45.2) |
| <i>Symptoms</i> | |
| Typical angina | 25 (25%) |
| Atypical angina | 49 (49%) |
| Chest pain | 22 (22%) |
| Dyspnea on exertion/fatigue | 5 (5%) |
| <i>Cardiovascular risk factors</i> | |
| Hypertension | 73 (72%) |
| Dyslipidemia | 80 (79%) |
| Diabetes | 39 (39%) |
| Smoking (past and current) | 34 (34%) |
| Current smoking | 14 (14%) |
| History of smoking | 20 (20%) |
| Family history of premature CAD | 21 (21%) |
| ≥ 2 cardiovascular risk factors | 85 (84%) |
| Systolic BP, mmHg (min-max) | 147 \pm 21.9 (99–184) |
| Diastolic BP, mmHg (min-max) | 78 \pm 10.8 (57–102) |
| Waist circumference, cm (min-max) | 98 \pm 10.3 (76–126) |
| Diamond-Forrester score (min-max) | 14.2 \pm 2.7 (9–20) |
| <i>Regular medication</i> | |
| On regular medication | 90 (89%) |
| Aspirin or clopidogrel | 54 (53%) |
| Statin | 66 (65%) |
| ACEI or ARB | 52 (51%) |
| Beta-blocker | 68 (67%) |
| Coronary calcium score, Agatston units (min-max) | 291 (0–5879) |
| ≤ 10 | 19 (19%) |
| 11–100 | 20 (20%) |
| 101–400 | 17 (17%) |
| 401–1000 | 26 (26%) |
| >1000 | 19 (19%) |
| <i>ICA</i> | |
| Any stenosis >40% | 54 (53%) |
| Any significant stenosis (FFR <0.80) | 44 (44%) |
| 1-vessel disease | 24 (24%) |
| 2-vessel disease | 12 (12%) |
| 3-vessel disease | 8 (8%) |
| Left main disease | 5 (5%) |

ACEI: angiotensin-converting enzyme inhibitor; ARB: angiotensin receptor blocker; BP: blood pressure; CAD: coronary artery disease; ICA: invasive coronary angiography.

Values are n (%) or mean \pm SD (95% confidence interval) (%) unless otherwise stated.

in cardiovascular CT (NF and NB). A modified American Heart Association 17-segment model was used for segmentation of the coronary arteries.²⁶ Each coronary segment was graded as normal, non-significant stenosis (<50%), 50–70% stenosis, $\geq 70\%$ stenosis/occlusion or uninterpretable. The effective radiation dose was calculated by multiplying the thoracic radiation factor ($k=0.014 \text{ mSv mGy}^{-1} \text{ cm}^{-1}$) by the dose-length product obtained for each acquisition.

Cardiac magnetic resonance perfusion imaging protocol

The CMR protocol was performed using a 1.5 T Siemens MAGNETOM Symphony TIM scanner (Siemens, Erlangen, Germany) with a 12-channel head coil (six anterior coils plus six spine coils in the patient table).²¹ No premedication was administered.

After acquisition of scout images in the orthogonal planes, three short-axis slices (basal, mid and apical) were planned. After 3 min of intravenous adenosine infusion ($140 \mu\text{g/kg/min}$) to achieve maximal hyperemia, a bolus of 0.07 mmol/kg gadobutrol (Gadovist, Bayer HealthCare Pharmaceuticals, Berlin, Germany) was injected at a rate of 4 ml/s with a power injector (Medrad Europe, Maastricht, The Netherlands). The first pass of gadolinium contrast in these slices was recorded over 50 cycles by a gradient echo sequence with a shared single saturation pre-pulse and during an end-expiratory breath hold. Typical sequence parameters were: TE 1.18 ms , TR 192 ms , TI 110 ms , flip angle 12° , slice thickness 10 mm ; FOV $290\text{--}460 \text{ mm}$, matrix $192 \text{ mm} \times 128 \text{ mm}$, spatial in-plane resolution $1.5\text{--}2.4 \text{ mm}$ and bandwidth 789 Hz per pixel. Any occurrence of symptomatic, hemodynamic or arrhythmic events during adenosine infusion was recorded. Shortly after the end of stress image acquisition, adenosine infusion was stopped.

For volumetric and functional assessment, long- and short-axis cine images were obtained using a steady-state free precession sequence with retrospective gating during an end-expiratory breath hold. Ten minutes after the first-pass gadolinium assessment, another acquisition was performed at rest with the same stress parameters. To achieve the full dose of 0.2 mmol/kg of gadolinium, the remaining 0.06 mmol/kg were then administered.

Ten minutes after the last contrast injection, delayed-enhanced images were acquired in breath-hold with a 2D phase-sensitive inversion-recovery sequence.

Cardiac magnetic resonance analysis

Tests were also blinded and evaluated by two independent readers with Society for Cardiovascular Magnetic Resonance (SCMR) level III training (AC and AS). When needed, a third reader, also with SCMR level III training (NB), acted to reach a consensus. Perfusion defects were defined as transmural or subendocardium-limited areas of lower signal intensity compared with adjacent healthy myocardium, lasting at least 10 frames. The stress and rest acquisitions were viewed simultaneously to better identify artefacts. In circumferential perfusion defects, the perfusion gradient from epicardium to endocardium was also assessed. Areas of hypoperfusion were matched to myocardial segments according

to the classic 17-segment model, excluding the apex as not being displayed in CMR perfusion imaging.²⁷ Each of the 16 segments was classified using a 4-point scoring system (from no defect to transmural defect). Late gadolinium enhancement was analyzed simultaneously, distinguishing inducible ischemia from scar. Isolated changes in myocardial kinetics or scarring without further ischemia were not considered as ischemia. Image quality and the interpreters' degree of trust were classified into four grades from poor to excellent and from very unsure to very confident, respectively.

Invasive coronary angiography and fractional flow reserve assessment

ICA and FFR assessment were performed according to standard techniques. Readers were unaware of CTA and CMR perfusion imaging data. When coronary segments with visual stenosis $>40\%$ were observed, a pressure wire (Certus, St. Jude Medical, MN, USA) was used to determine the corresponding FFR under steady-state hyperemia with intravenous adenosine infusion ($140 \mu\text{g/kg/min}$ over 3–6 minutes) using the RadiAnalyzer system (St. Jude Medical, MN, USA). Significant stenosis was defined as FFR <0.80 , occlusion or subocclusion, or $\geq 50\%$ left main stenosis.

Assignment of perfusion segments to the corresponding vascular territory

For vessel-based analysis, each myocardial segment with a perfusion defect on CMR perfusion imaging was matched to a major vascular territory: left anterior descending (LAD), circumflex (Cx) or right coronary artery (RCA). This association was carried out after checking ICA for the coronary anatomical pattern.

Noninvasive integration of anatomical and functional data

To assess the potential of integrated noninvasive anatomical and functional assessment, similar to the principle of the use of FFR in ICA, significant lesions were defined as $>50\%$ stenosis on CTA matched with a perfusion defect on CMR perfusion imaging in the corresponding segments. Less than 50% stenosis on CTA without perfusion defects on CMR perfusion imaging, and vice versa, were considered negative (see [Figure 2](#)).

Follow-up

Follow-up was completed for all patients, with a mean period of 2.9 ± 0.6 years ($0.3\text{--}3.8$ years). The follow-up was conducted by telephone and/or by letter. Data were collected regarding current health status and cardiovascular events, including death, acute coronary syndrome, elective and urgent coronary revascularization, stroke or unplanned hospitalization for heart failure or other cardiovascular causes.

Statistical analysis

The diagnostic performance of CTA and CMR perfusion imaging, alone and integrated, for the detection of

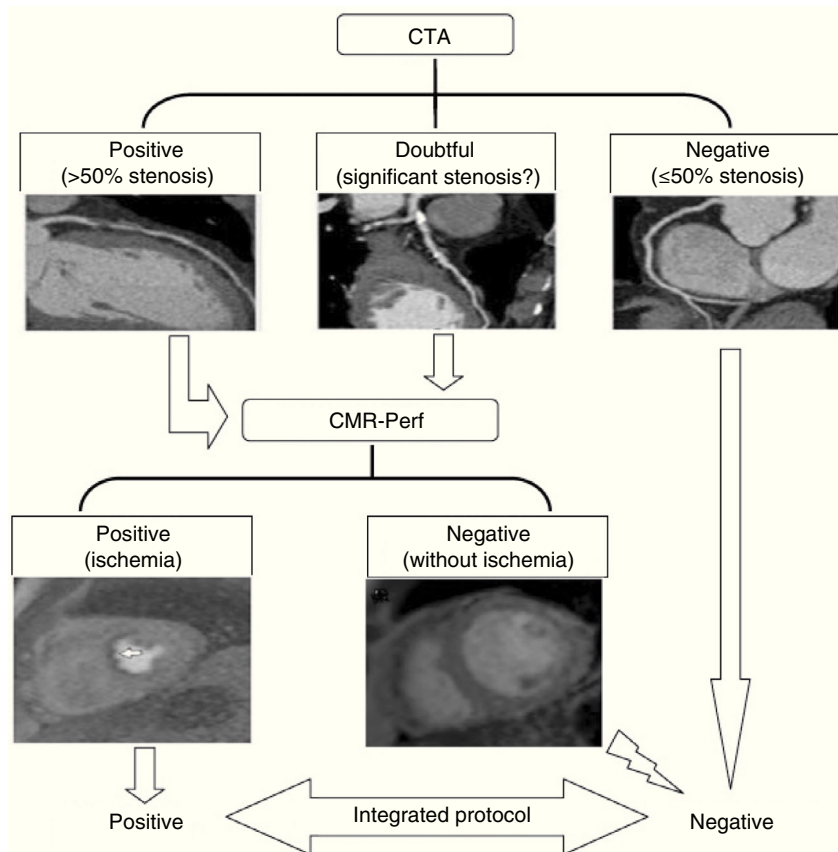


Figure 2 Algorithm for classification of stenosis by integration of CTA and CMR perfusion imaging data. CMR: cardiac magnetic resonance; CMR-Perf: cardiac magnetic resonance perfusion imaging; CTA: computed tomography angiography.

functionally significant CAD was compared using FFR as the reference standard. No segments interpretable by CTA were classified as positive for disease in isolated analysis, but when integrated they were considered positive or negative according to the perfusion data. All continuous variables were expressed as mean \pm standard deviation, while categorical variables were expressed as a percentage. The McNemar test was used to calculate the differences between proportions (sensitivity, specificity and accuracy) obtained from paired observations. Cohen's kappa was used to assess intermodality and intra- and interobserver variability. Receiver operating characteristic (ROC) curve analysis was used to compare the diagnostic accuracy and prediction of revascularization of CTA and CMR perfusion imaging, alone or integrated. Areas under the curve (AUCs) were compared using DeLong's method.²⁸

Statistical analyses were performed using SPSS version 18.0 (SPSS, Chicago, IL, USA) and MedCalc for Windows, version 12.7.7 (MedCalc Software, Ostend, Belgium). A *p* value <0.05 was considered statistically significant.

Results

All patients completed the study protocol without adverse effects. CTA and CMR perfusion imaging scans were performed within 9 ± 8.2 days before ICA. Table 1 summarizes the baseline characteristics and invasive cardiovascular risk stratification of the study population.

Computed tomography angiography results

Image quality was rated poor in nine patients, moderate in 39, good in 52 and excellent in one, and readers were unsure in 49 cases, confident in 47 and very confident in five. Mean radiation exposure in the CTA protocol, including coronary calcium scoring, was 5.47 ± 0.96 mSv. Thirty-three (33%) patients had at least one non-interpretable segment, often due to the presence of extensive calcification. Among patients who had fully interpretable scans, 10 had no atherosclerotic disease, 25 had mild disease ($<50\%$ stenosis) and 33 had $\geq 50\%$ stenosis. When non-interpretable segments were recorded as having significant CAD, 65 patients were classified as having significant CAD.

Cardiac magnetic resonance perfusion imaging results

Image quality was rated poor in two patients, moderate in 20, good in 57 and excellent in 22, and readers were unsure in the diagnosis of eight patients, confident in 60 and very confident in 33. Forty-six patients (70 out of 303 vascular territories) showed perfusion defects suggestive of ischemia during vasodilator stress. Thirty were within the LAD territory, 15 in the Cx territory and 25 in the RCA territory. Sixteen patients had late gadolinium enhancement compatible with ischemic etiology. Intra- and inter-observer

variability was good, with kappa values of 0.71 and 0.57, respectively.

Mean left ventricular ejection fraction was $65.4 \pm 10.8\%$.

Fractional flow reserve results

Fifty-four patients with $>40\%$ visually estimated stenosis were considered for FFR assessment. Coronary arteries with mild ($\leq 40\%$) disease (29 vessels) or without plaque (179 vessels) did not undergo FFR measurement. Also, vessels with luminal diameter <2 mm (10 vessels) were excluded. Nineteen totally occluded vessels and 11 vessels with subocclusion did not undergo FFR measurement and were regarded as positive. Additionally, FFR measurement was not performed in nine vessels with long lesions and severely calcified and tortuous or decreased flow after intra-coronary nitrate injection (TIMI flow ≤ 2). It was also not measured in five patients with left main disease because the potential risk was perceived as excessive. Lesions in which FFR could not be measured for the above reasons were considered positive for comparative purposes. In total, 36 non-occluded vessels (27 patients) were assessed by FFR.

Using this approach, 72 arteries were classified as positive, with a diagnosis of CAD in 44 patients (43.6% of the population): 24 with 1-vessel disease, 12 with 2-vessel disease and eight with 3-vessel disease.

Follow-up events

In the follow-up only three major cardiovascular adverse events (three patients) occurred: one acute coronary syndrome with concomitant urgent revascularization and two deaths (one from cardiovascular cause). Thirty-six patients (35.6% of the sample) were referred for coronary revascularization, 23 (63.8%) by percutaneous coronary angioplasty and 13 (36.1%) by surgery. Two revascularized patients had no functionally significant disease by FFR and CMR perfusion imaging, and the decision was based on purely anatomical findings.

Patient-based analysis

Diagnostic assessment by CTA had excellent sensitivity and NPV (100%) for functionally significant CAD. As expected, the specificity and PPV were comparatively low (61% and 67%, respectively).

Of the 46 patients with perfusion defects suggestive of ischemia on CMR perfusion imaging, 39 presented functionally significant disease in the invasive assessment. Of the 55 patients with negative CMR perfusion imaging exams, 50 were true negatives. CMR perfusion imaging had good diagnostic performance, with sensitivity of 89% and specificity of 88%, and with PPV of 85% and NPV of 91%.

When CTA and CMR perfusion imaging were integrated (CT+CMRint), sensitivity and NPV remained high (89% and 92%, respectively) compared with CMR perfusion imaging alone. Specificity and PPV increased considerably (95% and 93%, respectively). However, the differences in specificity were not statistically significant ($p=0.1250$). Four patients without disease on invasive assessment and with perfusion

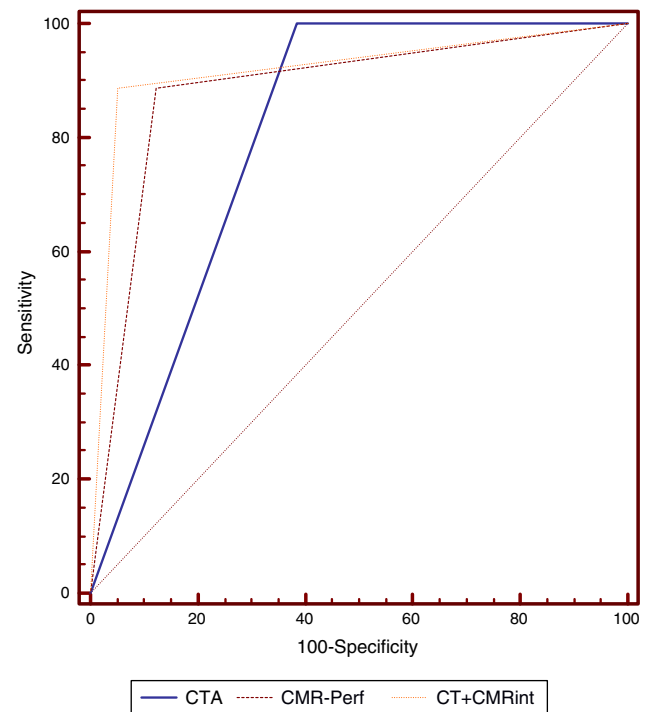


Figure 3 Receiver operating characteristic curve analysis of diagnostic accuracy of the different protocols with fractional flow reserve ≤ 0.80 as reference. CMR-Perf: cardiac magnetic resonance perfusion imaging; CT+CMRint: integrated CTA and CMR perfusion imaging; CTA: computed tomography angiography.

defects on CMR perfusion imaging were correctly reclassified as not having $>50\%$ stenosis on CTA, while 19 of 22 patients without significant disease by an invasive approach and at least one vessel with $>50\%$ stenosis on CTA were correctly reclassified as not having significant functional CAD since they had no compatible perfusion defects on CMR perfusion imaging.

Diagnostic accuracy for detection of CAD with functional significance by FFR as reference was 78% for CTA, 88% for CMR perfusion imaging and 92% for CT+CMRint. When C-statistics were calculated to compare the diagnostic accuracy of the various methods, the integrated protocol showed statistically significant superiority to predict functionally significant CAD by FFR (AUC=0.917, 95% CI: 0.85–0.96) compared with either CTA (AUC=0.807, 95% CI: 0.72–0.88, $p=0.0057$) or CMR perfusion imaging (AUC=0.882, 95% CI: 0.80–0.94, $p=0.0398$) alone (Figure 3).

Patient-based performances are summarized in Tables 2 and 3.

Vessel-based analysis

A total of 303 vessels (101 patients) were analyzed. CTA had greater sensitivity and NPV than CMR perfusion imaging in the detection of functionally significant CAD (95% vs. 79% and 97% vs. 93% respectively). With regard to specificity and PPV, CMR perfusion imaging performed better (93% vs. 67% and 79% vs. 48%, respectively). CMR perfusion imaging tended to perform better (AUC=0.87, 95% CI: 0.82–0.90) than CTA

Table 2 Comparison of diagnostic protocols in predicting functionally significant CAD.

| | TP | TN | FP | FN | Sen | Spe | PPV | PNV | +LR | −LR | DA |
|----------------------|----|-----|----|----|--------------|------------|------------|--------------|-------|------|------------|
| <i>Patient-based</i> | | | | | | | | | | | |
| CTA | 44 | 35 | 22 | 0 | 100 (92–100) | 61 (55–61) | 67 (61–67) | 100 (89–100) | 2.59 | 0.00 | 78 (71–78) |
| CMR-Perf | 39 | 50 | 7 | 5 | 89 (79–95) | 88 (80–93) | 85 (75–91) | 91 (83–96) | 7.22 | 0.13 | 88 (79–94) |
| CT+CMRint | 39 | 54 | 3 | 5 | 89 (75–96) | 95 (85–99) | 93 (81–89) | 92 (81–87) | 16.8 | 0.12 | 92 (84–96) |
| <i>Vessel-based</i> | | | | | | | | | | | |
| CTA | 69 | 155 | 75 | 4 | 95 (87–98) | 67 (65–69) | 48 (44–50) | 97 (94–99) | 2.90 | 0.08 | 74 (70–76) |
| CMR-Perf | 58 | 215 | 15 | 15 | 79 (71–86) | 93 (91–96) | 79 (71–86) | 93 (91–96) | 12.18 | 0.22 | 90 (86–93) |
| CT+CMRint | 55 | 221 | 9 | 18 | 75 (64–85) | 96 (93–98) | 86 (75–93) | 92 (88–95) | 19.25 | 0.26 | 91 (87–94) |

CMR-Perf: cardiac magnetic resonance perfusion imaging; CTA: computed tomography angiography; CT+CMRint: integrated computed tomography and cardiac magnetic resonance perfusion imaging; DA: diagnostic accuracy; FN: false negative; FP: false positive; NPV: negative predictive value; PPV: positive predictive value; Sen: sensitivity; Spe: specificity; TN: true negative; TP: true positive; +LR: positive likelihood ratio; −LR: negative likelihood ratio.

Values for sensitivity, specificity, PPV, and NPV and accuracy are presented with 95% CI.

(AUC=0.81, 95% CI: 0.79–0.88, p=0.0811) and the integrated protocol (AUC=0.84, 95% CI: 0.75–0.85, p=0.3510), but without statistical significance.

Vessel-based performances are summarized in [Tables 2 and 4](#).

Prediction of revascularization in follow-up

ROC curves were also constructed to test the ability of the various modalities to predict the occurrence of coronary revascularization during follow-up. The integrated protocol (AUC=0.824, 95% CI: 0.70–0.87) had superior performance compared to CTA (AUC=0.769, 95% CI: 0.68–0.85, p=0.5979) and CMR perfusion imaging (AUC=0.794, CI 95%: 0.70–0.87,

p=0.0405) alone, and was statistically significant for the latter.

However, as surgical revascularization was not triggered by FFR targets, anatomical assessment had more influence compared to functional data.

Discussion

Our study shows that integrating noninvasive functional and anatomic data from different modalities improves diagnostic accuracy, increasing specificity and PPV, using the current method of choice, FFR assessment, as reference.²⁴ The advantage of this integrated approach is that perfusion data can assess the functional significance of lesions depicted by CTA and, on the other hand, CTA can eliminate the false positives of perfusion scans.

Similar claims have been reported in the literature, although they are mainly confined to the combination of CTA with PET and SPECT, and more recently with CTP.^{19,20,22,24} However, in addition to their use of ionizing radiation, the clinical accessibility and prognostic value of these combinations are limited.

In the MARCC study by Groothuis et al., the combined use of CTA and myocardial perfusion imaging was evaluated in a population of 192 patients with low to intermediate pre-test probability of CAD, also using FFR as reference.¹⁶ The combination of the two techniques improved specificity and diagnostic accuracy (94% and 91%) with statistical significance compared to CTA (39% and 57%, p=0.0001) and CMR perfusion imaging (82% and 83%, p=0.016) alone. This approach also allowed recognition of other clinically relevant non-cardiac findings in 29 patients (15.1%). The main limitation of the study is that patients without disease on CTA did not undergo ICA, though this was partially mitigated by the absence of cardiovascular events in this group during a follow-up of 18 months. At the same time, review by FFR was limited to lesions with an estimated 30–70% luminal diameter, with all lesions >70% considered hemodynamically significant, which is inconsistent with current knowledge.^{7,8,25} The prevalence of significant CAD in patients referred for ICA in the MARCC study was also lower (29.5% vs. 43.1%) and CTA had a relatively poor performance

Table 3 Diagnostic accuracy of diagnostic protocols in predicting functionally significant disease (fractional flow reserve ≤0.80).

| Modality | AUC | 95% CI | p* |
|-----------|-------|-------------|--------|
| CTA | 0.807 | 0.716–0.879 | 0.0057 |
| CMR-Perf | 0.882 | 0.802–0.938 | 0.0398 |
| CT+CMRint | 0.917 | 0.845–0.963 | – |

AUC: area under the curve; CI: confidence interval; CMR-Perf: cardiac magnetic resonance perfusion imaging; CTA: computed tomography angiography; CT+CMRint: integrated computed tomography and cardiac magnetic resonance perfusion imaging.

* Compared with CT+CMRint.

Table 4 Comparison of diagnostic protocols in predicting coronary revascularization during follow-up.

| Modality | AUC | 95% CI | p* |
|-----------|-------|-------------|--------|
| CTA | 0.769 | 0.675–0.847 | 0.5979 |
| CMR-Perf | 0.794 | 0.702–0.868 | 0.0405 |
| CT+CMRint | 0.824 | 0.736–0.893 | – |

AUC: area under the curve; CI: confidence interval; CMR-Perf: cardiac magnetic resonance perfusion imaging; CTA: computed tomography angiography; CT+CMRint: integrated computed tomography and cardiac magnetic resonance perfusion imaging.

* Compared with CT+CMRint.

(diagnostic accuracy of 57% and specificity of 39%). In our study, CTA showed excellent performance (diagnostic accuracy of 78% and specificity of 61%), further highlighting the advantages of integration with CMR perfusion imaging.

Unlike other hybrid techniques, this protocol shows potential for greater accessibility in clinical practice, in addition to the strength of the evidence regarding the role of CTA and CMR perfusion imaging in assessing CAD.^{2-4,13-15} Moreover, assessment of heart disease in general and of extracardiac conditions by CTA and CMR perfusion imaging may become a powerful tool, with benefits for both patients and healthcare systems.^{16,29,30} As CT and CMR are expected to continue to evolve rapidly, it is conceivable that in the near future only one noninvasive test, including anatomical and functional assessment, will provide all the clinical information needed to diagnose and manage CAD.

Our study has several limitations. It is single-center, the number of patients is low and patients with known CAD were excluded. To validate our results, larger and broader samples are needed. As expected in standard clinical practice, anatomical assessment had the major influence and reduced the impact of functional assessment alone or combined when coronary revascularization was used as an endpoint. The size of the sample did not allow for collection of prognostic data during follow-up. Furthermore, the cost implications for health care systems also requires assessment. In the real world, referral of patients without lesions on CTA for CMR perfusion imaging could be avoided, given its excellent NPV. Since the study population was also used to study the additional value of CTP, image acquisition was suboptimal with regard to the assessment of coronary anatomy. Even so, as mentioned above, CTA had excellent performance. Finally, lesions were not assessed by FFR in all coronary segments with stenosis due to the underlying risk assessed by the interventional cardiologist, which limits our benchmark for significant CAD. However, this limitation applies to all studies involving FFR assessment since, for ethical reasons, patients cannot be subjected to procedures in which the risk outweighs the likely benefit.

Conclusion

Our study shows the advantages of integrating noninvasive anatomical and functional assessment based on CTA and CMR perfusion imaging, tests extensively validated in the literature. The increased specificity and PPV attained may lead to a considerable reduction in the use of invasive procedures for the diagnosis of CAD by limiting them to cases in which revascularization is planned, thus reducing risk and increasing patient comfort.

Conflicts of interest

The authors have no conflicts of interest to declare.

Disclosures

The first author received a grant from the Portuguese Society of Cardiology for advanced cardiovascular imaging training in the Cardiology Department of Centro Hospitalar de Vila Nova de Gaia/Espinho. This work, previously unpublished,

was awarded the Portuguese Society of Cardiology's Delta Ischemic Cardiomyopathy Prize for 2014.

Acknowledgments

The first author would like to thank the Portuguese Society of Cardiology for its support and the Cardiology Department of Centro Hospitalar de Vila Nova de Gaia/Espinho for their welcome, guidance and kindness during his fellowship. In particular, he would like to thank the Department of Advanced Cardiovascular Imaging, including his tutors, Dr Nuno Bettencourt and Dr Nuno Ferreira, and radiographers Daniel Leite, David Monteiro, Mónica Carvalho, Nuno Almeida, Pedro Rodrigues and Wilson Ferreira, as well as all the nurses involved.

References

1. Patel MR, Peterson ED, Dai D, et al. Low diagnostic yield of elective coronary angiography. *N Engl J Med.* 2010;362:886-95.
2. Chow BJ, Small G, Yam Y, et al. Incremental prognostic value of cardiac computed tomography in coronary artery disease using CONFIRM: COroNary computed tomography angiography evaluation for clinical outcomes: an International Multicenter registry. *Circ Cardiovasc Imaging.* 2011;4:463-72.
3. Pontone G, Andreini D, Bartorelli AL, et al. A long-term prognostic value of CT angiography and exercise ECG in patients with suspected CAD. *JACC: Cardiovasc Imaging.* 2013;6:641-50.
4. Vanhoenacker PK, Heijnenbroek-Kal MH, Van Heste R, et al. Diagnostic performance of multidetector CT angiography for assessment of coronary artery disease: meta-analysis. *Radiology.* 2007;244:419-28.
5. Vavere AL, Arbab-Zadeh A, Rochitte CE, et al. Coronary artery stenoses: accuracy of 64-detector row CT angiography in segments with mild, moderate, or severe calcification - a sub-analysis of the CORE-64 trial. *Radiology.* 2011;261:100-8.
6. Miller JM, Rochitte CE, Dewey M, et al. Diagnostic performance of coronary angiography by 64-row CT. *N Eng J Med.* 2008;359:2324-36.
7. Meijboom WB, Van Mieghem CA, van Pelt N, et al. Comprehensive assessment of coronary artery stenoses: computed tomography coronary angiography versus conventional coronary angiography and correlation with fractional flow reserve in patients with stable angina. *J Am Coll Cardiol.* 2008;52:636-43636.
8. Fischer JJ, Samady H, McPherson JA, et al. Comparison between visual assessment and quantitative angiography versus fractional flow reserve for native coronary narrowings of moderate severity. *Am J Cardiol.* 2002;90:210-5.
9. Balachandran KP, Berry C, Norrie J, et al. Relation between coronary pressure derived collateral flow, myocardial perfusion grade, and outcome in left ventricular function after rescue percutaneous coronary intervention. *Heart.* 2004;90:1450-4.
10. Pijls NH, Fearon WF, Tonino PA, et al. Fractional flow reserve versus angiography for guiding percutaneous coronary intervention in patients with multivessel coronary artery disease: 2-year follow-up of the FAME study. *J Am Coll Cardiol.* 2010;56:177-84.
11. Pijls NHJ, van Schaardenburgh P, Manoharan G, et al. Percutaneous coronary intervention of functionally nonsignificant stenosis: 5-year follow-up of the DEFER study. *J Am Coll Cardiol.* 2007;49:2105-11.
12. Donato P, Ferreira MJ, Silva V, et al. Cardiac magnetic resonance stress perfusion: a single-center study. *Rev Port Cardiol.* 2013;32:19-25.

13. Greenwood JP, Maredia N, Younger JF, et al. Cardiovascular magnetic resonance and single-photon emission computed tomography for diagnosis of coronary heart disease (CE-MARC): a prospective trial. *Lancet*. 2012;379:453–60.
14. Schwitter J, Wacker CM, van Rossum AC, et al. MR-IMPACT: comparison of perfusion-cardiac magnetic resonance with single-photon emission computed tomography for the detection of coronary artery disease in a multicentre, multivendor, randomized trial. *Eur Heart J*. 2008;29:480–9.
15. Schwitter J, Wacker CM, Wilke N, et al. MR-IMPACT II: Magnetic Resonance Imaging for Myocardial Perfusion Assessment in Coronary artery disease Trial: perfusion-cardiac magnetic resonance vs. single-photon emission computed tomography for the detection of coronary artery disease: a comparative multicentre, multivendor trial. *Eur Heart J*. 2013;34:775–81.
16. Groothuis JG, Beek AM, Brinckman SL, et al. Combined non-invasive functional and anatomical diagnostic work-up in clinical practice: the magnetic resonance and computed tomography in suspected coronary artery disease (MARCC) study. *Eur Heart J*. 2013;34:1990–8.
17. Bettencourt N, Ferreira N, Chiribiri A, et al. Additive value of magnetic resonance coronary angiography in a comprehensive cardiac magnetic resonance stress-rest protocol for detection of functionally significant coronary artery disease: a pilot study. *Circ Cardiovasc Imaging*. 2013;6:730–8.
18. Schuetz GM, Zacharopoulou NM, Schlattmann P, et al. Meta-analysis: noninvasive coronary angiography using computed tomography versus magnetic resonance imaging. *Ann Intern Med*. 2010;152:167–77.
19. Valenta I, Dilsizian V, Quercioli A, et al. Quantitative PET/CT measures of myocardial flow reserve and atherosclerosis for cardiac risk assessment and predicting adverse patient outcomes. *Curr Cardiol Rep*. 2013;15:344.
20. Kajander S, Joutsiniemi E, Saraste M, et al. Cardiac positron emission tomography/computed tomography imaging accurately detects anatomically and functionally significant coronary artery disease. *Circulation*. 2010;122:603–13.
21. Tashakkor AY, Nicolaou S, Leipsic J, et al. The emerging role of cardiac computed tomography for the assessment of coronary perfusion: a systematic review and meta-analysis. *Can J Cardiol*. 2012;28:413–22.
22. Bettencourt N, Rocha J, Ferreira N, et al. Incremental value of an integrated adenosine stress-rest MDCT perfusion protocol for detection of obstructive coronary artery disease. *J Cardiovasc Comput Tomogr*. 2011;5:392–405.
23. Rochitte CE, George RT, Chen MY, et al. Computed tomography angiography and perfusion to assess coronary artery stenosis causing perfusion defects by single photon emission computed tomography: the CORE320 study. *Eur Heart J*. 2013.
24. Techathit T, Cury RC. Stress myocardial CT perfusion: an update and future perspective. *JACC: Cardiovasc Imaging*. 2011;4:905–16.
25. Montalescot G, Sechtem U, Achenbach S, et al. 2013 ESC guidelines on the management of stable coronary artery disease: The Task Force on the management of stable coronary artery disease of the European Society of Cardiology. *Eur Heart J*. 2013;34:2949–3003.
26. Austen WG, Edwards JE, Frye RL, et al. A reporting system on patients evaluated for coronary artery disease. Report of the Ad Hoc Committee for Grading of Coronary Artery Disease, Council on Cardiovascular Surgery, American Heart Association. *Circulation*. 1975;51:5–40.
27. Cerqueira MD, Weissman NJ, Dilsizian V, et al. Standardized myocardial segmentation and nomenclature for tomographic imaging of the heart: a statement for healthcare professionals from the Cardiac Imaging Committee of the Council on Clinical Cardiology of the American Heart Association. *Circulation*. 2002;105:539–42.
28. DeLong ER, DeLong DM, Clarke-Pearson DL. Comparing the areas under two or more correlated receiver operating characteristic curves: a nonparametric approach. *Biometrics*. 1988;44:837–45.
29. Sousa C, Martins E, Pinho T, et al. Multiple coronary fistulae: characterization by multimodality imaging. *Rev Port Cardiol*. 2014;33:119–21.
30. Palomino AB, Estrada AP, Crespín MC, et al. Congenital complete absence of pericardium in a young woman with non-specific symptoms. *Rev Port Cardiol*. 2014;33, 249.e1–5.